Article

Introducing an Efficient In Vitro Cornea Mimetic Model for Testing Drug Permeability

Agnė Žiniauskaitė [1,2]**, Vytautas Cėpla** [3,4]**, Tadas Jelinskas** [4]**, Romuald Eimont** [3,4]**, Artūras Ulčinas** [4]**, Rūta Aldonytė** [2,3]**, Ramūnas Valiokas** [3,4]**, Giedrius Kalesnykas** [1,5] **and Jenni J. Hakkarainen** [5,*]

1   UAB Experimentica, Saulėtekio ave 7C, LT-10223 Vilnius, Lithuania; agne@experimentica.com (A.Ž.); gk@experimentica.com (G.K.)
2   State Research Institute Center for Innovative Medicine, Santariskiu 5, LT-08406 Vilnius, Lithuania; ruta.aldonyte@imcentras.lt
3   UAB Ferentis, Savanorių 231, LT-02300 Vilnius, Lithuania; vytautas@ferentis.eu (V.C.); romuald@ferentis.eu (R.E.); valiokas@ftmc.lt (R.V.)
4   Center for Physical Sciences and Technology, Department of Nanoengineering, Savanorių 231, LT-02300 Vilnius, Lithuania; tadas@ferentis.eu (T.J.); ulcinas@ftmc.lt (A.U.)
5   Experimentica Ltd., Microkatu 1, P.O. Box 1199, FI-70211 Kuopio, Finland
*   Correspondence: jenni@experimentica.com

Abstract: There is a growing need for novel in vitro corneal models to replace animal-based ex vivo tests in drug permeability studies. In this study, we demonstrated a corneal mimetic that models the stromal and epithelial compartments of the human cornea. Human corneal epithelial cells (HCE-T) were grown on top of a self-supporting porcine collagen-based hydrogel. Cross-sections of the multi-layers were characterized by histological staining and immunocytochemistry of zonula occludens-1 protein (ZO-1) and occludin. Furthermore, water content and bssic elastic properties of the synthetized collagen type I-based hydrogels were measured. The apparent permeability coefficient (P_{app}) values of a representative set of ophthalmic drugs were measured and correlated to rabbit cornea P_{app} values found in the literature. A multilayered structure of HCE-T cells and the expression of ZO-1 and occludin in the full thickness of the multilayer were observed. The hydrogel-based corneal model exhibited an excellent correlation to rabbit corneal permeability (r = 0.96), whereas the insert-grown HCE-T multilayer was more permeable and the correlation to the rabbit corneal permeability was lower (r = 0.89). The hydrogel-based human corneal model predicts the rabbit corneal permeability more reliably in comparison to HCE-T cells grown in inserts. This in vitro human corneal model can be successfully employed for drug permeability tests whilst avoiding ethical issues and reducing costs.

Keywords: in vitro corneal model; collagen hydrogel; permeability

1. Introduction

The topical administration of ophthalmic drugs remains the preferred route of drug delivery to ocular tissues. However, the poor bioavailability of drugs often limits their efficacy. The cornea decreases drug bioavailability due to its complex layered structure comprising of a stratified epithelium, Bowman's layer, stroma, Descemet's membrane, and, finally, the endothelial layer. The corneal epithelium itself is composed of layered squamous, wing, and basal cells. The superficial apical layer of the epithelial cells contains tight junctions that seal the intercellular spaces between them, making the corneal epithelium into an efficient diffusion barrier. Therefore, the corneal epithelium represents a rate-limiting barrier for topically administered hydrophilic drugs and macromolecules. The corneal stroma consists mostly of water (~80%) and type I collagen fibrils and makes up to 90% of the thickness of the cornea [1,2]. Therefore, with these properties, the corneal stroma restricts the penetration of hydrophobic drug molecules effectively [1].

Directive 2010/63/EU of the European Parliament and the Council on the protection of animals used for scientific purposes strongly supports the development and validation of nonanimal methods and models [3]. Therefore, the ethical issues have become an important aspect for society, authorities, and scientists. However, excised animal corneas (ex vivo) are still being used for permeability testing [4–6]. There are many disadvantages in the use of animal ex vivo corneas, including the high numbers of animals being sacrificed and, subsequently, the high costs involved. Thus, innovative and validated in vitro methods are needed to replace the current ex vivo methods.

Three-dimensional (3D) corneal tissue models have been studied and described before [7,8]. These in vitro models offer faster, cheaper, and ethically more appropriate tools for drug development. However, the permeability data of clinically used ophthalmic drugs through these models are insufficient. To the best of our knowledge, very few 3D models of the human cornea with permeability datasets of a wide range of compounds have been published; however, the permeability properties of previously established models deviated from the permeability of rabbit corneas [9–11]. Moreover, cell-based corneal models are still at the early stages of development. Nevertheless, their promising potential for use in pharmacokinetic, penetration, and toxicity studies are driving research forward. Several types of cells have been used for in vitro cornea modeling, for example, epithelial cells [12–14], as well as epithelial cells cultured together with stromal cells [8–11]. The supporting matrix in corneal models is often collagen-based as it mimics the chemistry of the native corneal stroma where the collagen fibrils are enriched with proteoglycans [15,16].

There has been extensive research and development on the already established corneal in vitro models mentioned above. Nevertheless, the major drawback in most of the studies comparing in vitro data with excised animal corneas is the use of different-permeability apparatuses resulting in substantial differences in permeability coefficients [17]. Therefore, the aim of this study was to develop a self-supporting, stable, and transparent hydrogel platform. To reliably compare the permeability coefficients, such a testing platform would employ the regular permeability apparatus commonly used for most of the excised rabbit corneal permeation studies.

The technical challenge in developing disposable in vitro constructs compatible with the standard drug permeability instrumentation is the synthesis of stable hydrogel material without compromising its permeability and cell-supporting characteristics. Moreover, besides the (bio)chemical composition and the characteristic fibrous ultrastructure, the elasto-mechanic properties of the hydrogel must match those of the native corneal tissue, triggering the mechanobiological cues that facilitate efficient cellular multilayering [18]. Therefore, in this paper, we presented an in vitro corneal mimetic where a chemically crosslinked collagen-based, self-supporting hydrogel is employed as a matrix for a human corneal epithelial multilayer. Chemically crosslinked collagen hydrogels have emerged as an interesting class of biomaterials suitable for prosthesis fabrication and capable of inducing corneal regeneration [19]. Previous reports on porcine collagen-based hydrogels have indicated their corneal epithelial layer-promoting characteristics [20]. The permeability of this type of crosslinked collagen hydrogel has also been tested, and it was comparable to that of the corneal stroma in the case of cell nutrition molecules [20,21]. However, the drug permeabilities of a full cornea-mimicking construct comprising both the hydrogel and human corneal epithelial cell multilayer have not been studied. Therefore, herein, we report on the engineering of a human cornea-mimicking device compatible with established drug permeability analysis techniques. By employing it, we have performed quantitative assessment of the permeability of pharmacologically relevant ophthalmic drugs and compared it with the current in vitro and ex vivo standards, a human corneal epithelial multilayer grown in cell culture inserts and a rabbit cornea, respectively. A high correlation in permeability properties of our corneal mimetic was achieved with the rabbit cornea, enabling further translation of this in vitro system into the pharmaceutical field and the successful replacement of conventionally used excised rabbit tissues.

2. Materials and Methods

2.1. Synthesis and Characterization of Hydrogels

Collagen hydrogel membranes were synthesized from chemically crosslinked porcine collagen type I (NMP collagen PS, Nippon Meatpackers, Ibaraki, Japan) adapting the published protocol [20]. Briefly, collagen at 12% (*w/w*) in aqueous solution was crosslinked with 4-(4,6-dimethoxy-1,3,5-triazin-2-yl)-4-methylmorpholinium chloride (DMTMM, Merck KGaA, Darmstadt, Germany) [22]. The amine molar ratio of collagen-NH_2 to DMTMM was 1:1. After thoroughly mixing, the final solution containing $8.5 \pm 0.3\%$ collagen was casted onto a plastic circular supporting frame made from poly-L-lactic acid (PLLA). The external diameter of the frame was 19.6 ± 0.6 mm, the inner diameter (corresponding to the diameter of the hydrogel membrane) was 10.8 ± 0.4 mm, and the thickness was 0.8 ± 0.1 mm. The obtained hydrogel membranes in the frames were left to cure overnight in a 100% humid atmosphere. After curing, the hydrogel membranes were washed several times with 0.1 M of phosphate buffer (PB, pH 7.4) and kept in 0.1 M of PB supplemented with 100 U/mL of penicillin, 100 µg/mL of streptomycin, and 0.25 µg/mL of Fungizone (Gibco, Thermo Fischer Scientific, Waltham, MA, USA) until use.

The elastic (Young's) moduli E of the synthesized hydrogel membranes were determined by the atomic force microscopy (AFM) nanoindentation technique [23,24]. The spring constant of tipless AFM cantilevers (NSC36-B, MicroMasch, Sofia, Bulgaria) was calibrated using the thermal noise method [25], before the attachment of a microsphere, and was found to be 4.0 ± 0.6 N/m. For hydrogel analysis, the probes from the same synthesis batch were chosen because of the observed low variation in the spring constant values. To control the geometry of the contact, SiO_2 microspheres with a diameter of 6.65 ± 0.28 µm (Microparticles GmbH, Berlin, Germany) were attached to the AFM cantilevers using UV-curable glue (NOA68, Norland, Cranbury, NJ, USA), taking care to control the amount of glue on the cantilever. The attachment of the microspheres and their diameters were inspected by optical microscopy (a $50\times$ lens, BX51, Olympus, Japan). The measured diameter was 6.65 ± 0.15 µm, matching the data provided by the manufacturer.

To avoid the movement of the sample during the AFM elastic modulus measurement, the hydrogel membranes (cutouts with a typical width of 3 mm and a length of 5 mm) were attached to (3-aminopropyl)trimethoxysilane-treated glass substrates (BaltFab, Vilnius, Lithuania) via glutaraldehyde chemistry. The hydrogel membrane was placed in a small Petri dish filled with phosphate-buffered saline (PBS, pH 7.4) and mounted onto the stage of an inverted optical microscope (IX73, Olympus, Japan), which served as a base for the AFM instrument (Nanowizard 3, JPK, Berlin, Germany). The detection sensitivity factor was determined from the force–displacement curve by approaching the glass surface. The typical detection sensitivity values were 10–20 nm/V. The probe was then repositioned onto the hydrogel membrane and 1024 force curves were collected (50×50 µm area) in the Quantitative Imaging™ (QI) mode with a force setpoint of 120 nN and a loading rate of 50 µm/s. This procedure was repeated at four different locations for each hydrogel membrane analyzed. The E values of the hydrogel samples were extracted by fitting the approach part of the force–displacement curve with the Hertz sphere-on-plane elastic contact model (JPK data processing software, version spm-5.0.84). The elastic moduli E were calculated from the analysis of three different synthesis batches of four hydrogel membranes (12 samples in total).

2.2. Cell Culture of Human Corneal Epithelial Cells

The human corneal epithelial cell line (HCE-T) [26] was purchased from the RIKEN BRC Cell Engineering Division, cell bank (Tsukuba, Japan). The cells were grown in Dulbecco's modified Eagle's medium/nutrient mixture F-12 (1:1), 5% fetal bovine serum, penicillin (100 U/mL), streptomycin (100 µg/mL), insulin (5 µg/mL), human recombinant epidermal growth factor (10 ng/mL) (all from Gibco, Thermo Fischer Scientific), and 0.5% dimethyl sulfoxide (Sigma-Aldrich, St. Louis, MO, USA) in an incubator with a humidified atmosphere of 5% CO_2 and a temperature of 37 °C [27]. The cell suspension was applied

on the top of the collagen hydrogel membranes fixed in their supporting frames and placed into 6-well cell culture plates (Cellstar®, Greiner Bio-One, Kremsmünster, Austria). The seeding density was 50,000 cells/cm^2 and the cells were allowed to attach for 20 min prior to filling the wells with media. Cultures were maintained in 5% CO$_2$ at 37 °C for one week. Thereafter, the HCE-T layer was cultured at the air–liquid interface by lifting the collagen hydrogels, with their supporting frames, onto permeable cell culture inserts with a diameter of 30 mm (Millicell, Sigma-Aldrich). Culture medium was added at the basolateral side of the insert membrane and was changed three times a week, and the cultures were further maintained for two weeks. Control HCE-T cultures were seeded directly onto permeable (0.4 μm pores) cell culture inserts (Corning® Costar® Snapwell, 12 mm, Corning, NY, USA), cultured until confluence for one week, and then stratified for three weeks at the air–liquid interface, as described previously [28].

2.3. Permeability Testing

Selection criteria for the ophthalmic drugs and reference molecules (Table 1) tested in this study were as follows: (1) availability of rabbit corneal permeability values from the literature with a wide range of permeabilities, (2) clinically used ophthalmic drug molecules with different mechanisms of action, (3) generally used fluorescent reference molecules, and (4) lipophilic, hydrophilic, and high-molecular-weight molecules. The cytotoxicity of the drug molecules, at the selected test concentrations (Table 1), was assessed for 4 h using a resazurin cell viability assay, as previously described [27].

Table 1. Ophthalmic drugs and reference molecules tested in the permeability experiments.

Ophthalmic Drug/Reference Molecule	Supplier	Concentration Tested
6-carboxyfluorescein (6-CF)	Sigma-Aldrich	50 μM
Rhodamine B (Rho B)	Sigma-Aldrich	50 μM
FITC-dextran, 4 kDa (FD4)	Sigma-Aldrich	50 μM
FITC-dextran, 70 kDa (FD70)	Sigma-Aldrich	200 μg/mL
Rhodamine 123 (Rho 123)	Sigma-Aldrich	10 μM
Betaxolol (Beta)	Cayman Chemicals	10 μM
(+)-Pilocarpine HCl (Pilo)	Cayman Chemicals	10 μM
Timolol maleate (Timo)	Cayman Chemicals	10 μM
Chloramphenicol (Chlora)	BioChemica, AppliChem	80 μM
Dexamethasone (Dexa)	Cayman Chemicals	100 μM
Brinzolamide (Brinzo)	Cayman Chemicals	89 μM

The permeability experiments were conducted in a NaviCyte vertical chamber system (Harvard Apparatus, Holliston, MA, USA). Briefly, the cell layers or rabbit corneas with the scleral rim were washed, equilibrated in pre-warmed BSS Plus buffer (Alcon, Fort Worth, TX, USA) for 15 min, and then placed between the donor and receiver chambers. The donor chamber was filled with 5.5 mL of donor solution and the receiver chamber was filled with 6.5 mL of BSS Plus to mimic the intraocular pressure in the receiver chamber. Solutions in the chambers were mixed individually using carbogen (95% oxygen and 5% carbon dioxide) gas. The samples were collected from the receiver chambers at 10, 15, 30, 45, 60, 90, and 120 min and the samples from the donor chambers were collected at 30, 60, 90, and 120 min for in vitro corneal models. The samples were collected from the receiver chambers at 30, 60, 120, 150, 180, 210, and 240 min and the samples from the donor chambers were collected at 0, 60, 180, and 240 min for the rabbit corneas. The sample concentrations of the fluorescent molecules (FD4, FD70, Rho 123, Rho B, and 6-CF) were quantified in the 96-well plates using a Cytation 3 multi-mode reader (BioTek Instruments, Winooski, VT, USA). A minimum of five cell inserts were used to test the permeability of the clinically used ophthalmic drugs and fluorescent reference molecules listed in Table 1. The permeability of fluorescent reference molecules (FITC-dextran 4 kDa, 6-carboxyfluorescein, Rhodamine 123, and Rhodamine B) was tested across rabbit corneas, with a minimum of

four corneas used per molecule. The results obtained for the corneal model with collagen hydrogel and for the cell layers grown in cell culture inserts were compared with the permeability results of rabbit corneas from existing published studies supplemented with data obtained in this study.

2.4. Quantification of Brinzolamide, Dexamethasone, Chloramphenicol, Timolol, Pilocarpine, and Betaxolol

The samples collected from receiver and donor chambers in permeability tests were prepared for analysis by protein precipitation using the one-fold dilution of acetonitrile, followed by centrifugation for pellet compaction. For quantification of model drug concentrations, analytical ultra-performance liquid chromatography (UPLC) with MS/MS detection was used. The instrumentation consisted of a Thermo Vanquish Horizon UPLC + Thermo Quantis triple quadrupole MS with an HSS T3 column (1.8 μm, 2.1 × 30 mm) (Waters Corporation, Milford, MA, USA). For each analyte, separate nine-point calibration curves (1–10,000 nM) were prepared using the BSS Plus buffer. In addition, blank, zero samples, and quality control samples (50, 500, and 5000 nM) were analyzed. For dexamethasone, chromatographic separation was performed using gradient elution with (A) 2 mM of ammonium formate (pH 8.5) and (B) acetonitrile. For brinzolamide, chloramphenicol, timolol, pilocarpine, and betaxolol, chromatographic separations were preformed using gradient elution with (A) 2 mM of ammonium formate (pH 8.5) and (B) methanol as follows: 0–0.5 min: 2% B; 0.5–1.0 min: 2% B → 80% B; 1.0–1.75 min: 80% B → 98% B; 1.75–2.25 min: 98% B → 2% B. The flow rate was 0.65 mL/min, the column temperature was 40 °C, and the injection volume was 4 μL. The ionization conditions were as follows: nitrogen sheath (50 instrument units), auxiliary (4 instrument units), sweep gas flow rates (4 instrument units), and spray voltage 2 kV (ESI+) and 3.5 kV (ESI−). The following transitions were used for model drug detections: m/z 393 → 355 for dexamethasone, m/z 384 → 136 for brinzolamide, m/z 321 → 194 for chloramphenicol, m/z 317 → 244 for timolol, m/z 209 → 121 for pilocarpine, and m/z 308 → 121 for betaxolol. The internal standard method was used for the calculation of the concentration of the model drug using Xcalibur 4.1 software (Thermo Fischer Scientific).

2.5. Histology

After the permeability tests, the cell layers were washed three times with BSS Plus and fixed in methanol (Thermo Fischer Scientific, Waltham, MA, USA) at −20 °C for 20 min. A rabbit cornea was fixed in 4% paraformaldehyde (Sigma-Aldrich) at +4 °C overnight. After fixation, the samples were washed with PBS and embedded into an optimal cutting temperature O.C.T. medium (Tissue Tek®, Sakura Finetek USA, Torrance, CA, USA). The sections (5, 10, and 30 μm for HCE-T cells grown in the insert, rabbit cornea, and HCE-T cells grown on top of hydrogel, respectively) were cut using a cryostat (Leica CM1860, Leica Biosystems, Wetzlar, Germany) and collected on SuperFrost® (Thermo Fisher Scientific) slides and stored at −20 °C until further use. Sections were stained with hematoxylin (Sigma-Aldrich) and eosin (Merck Millipore, Darmstadt, Germany). The stained sections were then visualized under a light microscope (Leica DLMB 100S, Leica Microsystems, Wetzlar, Germany) equipped with the LAS EZ software (Leica).

2.6. Immunofluorescent Staining of Tight Junction Proteins

Cryosections were washed with PBS, permeabilized, and then blocked with 5% normal goat serum (NGS) (Biowest, Nuaille, France) and 0.5% Triton X-100 (Sigma-Aldrich) in PBS for 20 min. The sections were then incubated at +4 °C overnight with rabbit anti-zonula occludens-1 protein (ZO-1) antibody (dilution 1:100, Thermo Fisher Scientific) and mouse anti-occludin antibody (1:200, Thermo Fisher Scientific). Mouse IgG isotype control (Abcam plc, Cambridge, UK) was used as a negative control for rabbit tissue sections. After washing in 0.5% NGS in PBS, the sections were incubated with goat anti-rabbit secondary antibody, conjugated with Alexa Fluor 488 (1:500) or Alexa Fluor Plus 647 (1:500) or goat anti-mouse IgG1 secondary 488 (1:500) (Thermo Fischer Scientific) for 3 h, and washed

in PBS. Finally, nuclei were stained with 0.1 µg/mL of 4′,6-diamidino-2-phenylindole dihydrochloride (DAPI) (Sigma-Aldrich) for 30 min. The fluorescent images were acquired in an Axio Imager, on an ApoTome.2 fluorescence microscope (Carl Zeiss, Oberkochen, Germany) and Leica THUNDER 3D Tissue Imager (Leica Microsystems).

2.7. Data Analysis

The apparent permeability coefficient (P_{app}) value (cm/s), describing the rate at which molecule cross the barrier, was calculated using the following equation:

$$P_{app} = (\Delta Q_r / \Delta t) \, (1/(A C_d)),\tag{1}$$

where $\Delta Q_r / \Delta t$ is a slope of a linear region of the cumulative amount of the molecule in the receiver chamber versus time, A is the surface area available for diffusion, and C_d is the average concentration of the molecule in the donor chamber.

The mass balance (%) was calculated according to the following equation:

$$\text{Mass balance } (\%) = \frac{\left(C_{r(z)} * V_r\right) + \left(C_{d(z)} * V_d\right)}{(\text{average } C_d * V_d) * 100}\tag{2}$$

where C_r and C_d are the concentrations in receiver and donor chambers, respectively, at the end (z) of the permeability assay; V_r and V_d are the volumes of the receiver and donor chambers, respectively.

2.8. Statistical Analysis

All values are presented as mean ± standard error of the mean (SEM). Cytotoxicity and permeability data were analyzed using ordinary one-way-ANOVA followed by Dunnett's and Tukey's multiple comparisons post-hoc test, respectively, performed using GraphPad Prism (version 9.0.0, GraphPad Software, San Diego, CA, USA). Differences were considered to be statistically significant at $P < 0.05$ (* $P < 0.05$; ** $P < 0.01$; *** $P < 0.001$; **** $P < 0.0001$; ns = not significant).

Linear regression (R^2) and Pearson's correlation coefficient (r) analysis were performed using GraphPad Prism (version 9.0.0, GraphPad Software).

3. Results and Discussions

The aim of the present study was to establish an in vitro corneal mimetic with a collagen-based self-supporting hydrogel and to validate the model as an alternative for the ex vivo rabbit corneas in permeability testing. The permeability of drug molecules, marketed ophthalmic drugs with different physicochemical properties, was tested and compared to permeability values of rabbit corneal tissue.

The hydrogels, serving as the support for epithelial cells and mimicking the stromal layer of the native cornea, contained commercially available porcine collagen type I. It was chemically crosslinked into a self-supporting, transparent material following the procedures developed for the synthesis of artificial corneas in cornea transplantation [20]. The crosslinking agent (DMTMM) used in this study allowed obtaining a slower crosslinking rate and better overall hydrogel synthesis control as compared to N-hydroxysuccinimide (NHS)/1-ethyl-3-(3-dimethylaminopropyl)carbodiimide (EDC) crosslinking chemistry [29]. The measured elastic modulus of such synthesized collagen hydrogels was 0.36 ± 0.07 MPa. This is slightly lower than that of the collagen hydrogels crosslinked using NHS/EDC that displayed an elastic modulus of 0.60 ± 0.26 MPa [21]. It should be noted that the AFM nanoindentation technique used here directly measures the elastic modulus of the surface and sub-surface layers of less than 1 µm in depth, as compared to the bulk elastic moduli measured by other techniques (e.g., oscillatory rheology). Therefore, the AFM nanoindentation technique should yield a value that is arguably closer to the actual elasticity of the sample, as sensed by cells, especially in case of materials having a certain degree of heterogeneity. Our recent study on hydrogels, manufactured using collagen-like

peptide-based formulations, however, did not find a significant divergence between the results yielded by the AFM nanoindentation and oscillatory rheology [30]. We would like to point out that the synthesized collagen hydrogels employed in this study had certain physical differences as compared to the native human and rabbit cornea. The collagen hydrogels used contained $8.5 \pm 0.3\%$ collagen and $91.5 \pm 0.3\%$ water in comparison to a human and rabbit corneas water content of 78–79% [20,31]. However, it is known that other synthetic porcine and recombinant human collagen hydrogels exhibit higher water content (~90%, [20]). The elastic moduli of human and rabbit corneas (0.16–0.30 and 0.16–0.35 MPa, respectively [32]) are comparable to our collagen hydrogel, 0.36 ± 0.07 MPa. Also, the variation between the DMTMM crosslinked hydrogels samples employed in the current study was minimal, where the standard deviation of the 12 samples was only 0.07 MPa. Thus, homogeneous hydrogels were obtained showing negligible structural variations between the samples, a reproducibility that is important for forming consistent cell layer structures and the interpretation of results obtained from any drug testing performed on them.

The human and rabbit corneal stroma contains predominantly type I collagen [16,33], which has been shown to enhance the morphology and adhesion of HCE-T cells [34]. Therefore, collagen type I hydrogels were casted onto a supporting frame (Figure 1) and used to obtain the in vitro corneal mimetic, a multilayered human corneal epithelial layer. The supporting frame was designed to fit between the vertical chambers and to protect the cell layers grown onto the hydrogel during handling and mounting onto the device for permeability measurements. No signs of the cytotoxicity of the supporting frame were observed during the cell culture; cells were growing normally in close proximity of the supporting frame without any morphological alterations.
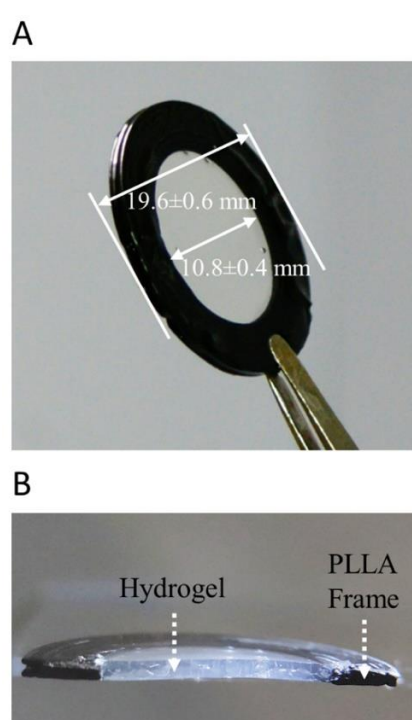
Figure 1. Collagen hydrogel casted onto a plastic circular supporting frame made from poly-L-lactic acid (PLLA, seen as black ring) designed to support the formation of a human corneal epithelial multilayer for drug permeability testing in a vertical chamber (**A**). Cross-section of the transparent hydrogel/plastic supporting frame (**B**).

The tested drug molecules (Table 1) did not show signs of cytotoxicity. No statistically significant difference ($P > 0.05$) in cell viabilities (between $93\% \pm 2\%$ and $98\% \pm 2\%$) compared to cell media control ($100\% \pm 2\%$) were found.

The characterization of the developed in vitro human corneal mimetic is shown in Figure 2. Both in vitro corneal models express ZO-1 (Figure 2A,B), which is responsible for anchoring integral proteins of tight junctions to the actin cytoskeleton [35]. Interestingly, ZO-1 and occludin are expressed in full thickness of in vitro multilayers (Figure 2D,E). It is well known that the tight junction barrier is only expressed in the superficial cell layer of the rabbit corneal epithelium (Figure 2F). This indicates that there are significant differences between in vitro and in vivo epithelial phenotypes.
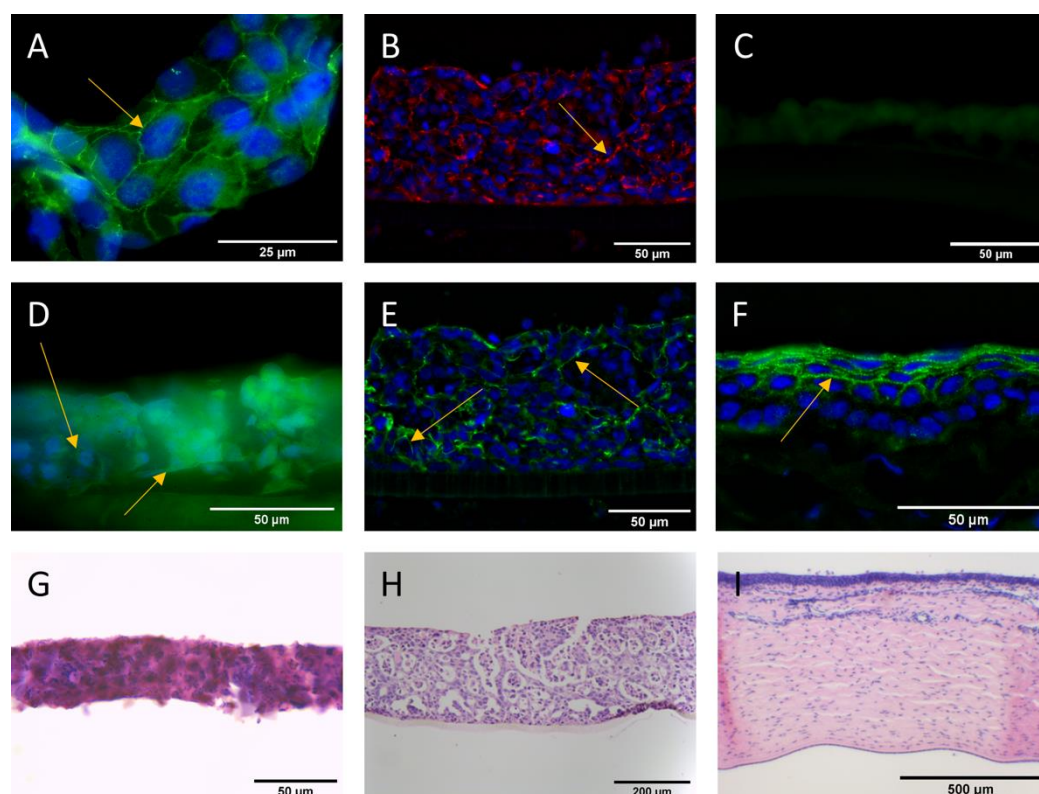
Figure 2. Immunocytochemistry and histology of in vitro corneal models and rabbit cornea. Immunofluorescent staining for zonula occludens-1 (ZO-1) protein expression (green) in HCE-T multilayers grown on top of the collagen hydrogel (**A**), human corneal epithelial cells (HCE-T) grown on conventional cell culture insert (red) (**B**). Negative control of occludin for HCE-T cells grown on top of hydrogel (**C**). Immunofluorescent staining for occludin (green) in hydrogel-based in vitro corneal mimetic (**D**), HCE-T cells grown in the insert (**E**), and rabbit cornea (**F**). Nuclei are stained with DAPI (blue) (**A**–**F**). Yellow arrows indicate the tight junctional staining between the cells. Hematoxylin and eosin-stained sections of HCE-T multilayers grown on top of the collagen hydrogel (**G**), HCE-T cells grown in the insert (**H**), and rabbit cornea (**I**).

Furthermore, both in vitro corneal models, cells grown in cell culture inserts and the in vitro corneal mimetic with the self-supporting hydrogel, exhibited multilayers of epithelial cells (Figure 2G,H). However, the cells grown in cell culture inserts demonstrated a much thicker (100–200 µm) epithelial cell multilayer than those grown on hydrogel (50 µm). The thickness of the epithelial cell multilayer in the hydrogel-based corneal mimetic model corresponds to the thickness of rabbit corneal epithelium (Figure 2I).

The apparent permeability coefficient (P_{app}) values for fluorescent reference molecules (6-CF, Rho B, Rho 123, FD4, and FD70) and for clinically used topically applied drugs (betaxolol, brinzolamide, dexamethasone, timolol maleate, pilocarpine, and chloramphenicol) were determined in the hydrogel-based model and on an insert-grown corneal multilayer that lacked a stromal equivalent. Tested molecules (Table 1) represent generally used lipophilic and hydrophilic molecules from the low- to high-molecular-weight range. The

P_{app} values obtained in this study and the reference values of rabbit corneal permeability from the literature are shown in Table 2.

Table 2. P_{app} values across the in vitro hydrogel-based human corneal model, cells grown in cell culture inserts, and rabbit cornea.

Test Molecule	Molecular Weight *	LogP	P_{app} (cm/s) $\times 10^6$ (Mean $\pm$ SEM)				Ref.
			Hydrogel-Based Human Corneal Model	Cells Grown in Inserts	Rabbit Cornea	Rabbit Cornea (Values from Literature)	
FITC-dextran 70 kDa	70,000	−3.29 #	0.16 ± 0.08	0.07 ± 0.01	nd	Impermeable	[36]
FITC-dextran 4 kDa	4000	−3.41 #	0.80 ± 0.52	1.43 ± 0.25	0.40 ± 0.09	0.056, 0.09	[10,37]
Rhodamine 123	380.8	1.06 %	0.96 ± 0.27	2.22 ± 0.05	0.42 ± 0.17	0.15	[38]
6-carboxy-fluorescein	376.3	−3.1 $	0.89 ± 0.16	2.87 ± 0.30	1.4 ± 0.2	0.46	[28]
Brinzolamide	383.5	−1.8 *	1.17 ± 0.36	8.99 ± 0.05	nd	0.2	[5]
Dexamethasone	392.5	1.83 *	6.86 ± 1.13	23.32 ± 0.20	nd	5, 7.7	[9,39]
Chloramphenicol	323.1	1.14 *	4.75 ± 0.39	12.79 ± 0.54	nd	6.8	[39]
Timolol maleate	316.4	1.1 *	29.47 ± 1.05	20.62 ± 4.27	nd	11.7, 22.5	[9,39]
Pilocarpine	208.3	1.1 *	16.86 ± 0.58	39.4 ± 0.97	nd	17.4	[39]
Rhodamine B	479.0	2.3 *	19.98 ± 2.47	40.22 ± 3.02	9.1 ± 0.9	13.5, 18.1	[10,28]
Betaxolol	307.4	2.81 *	34.56 ± 3.69	42.00 ± 3.66	nd	27	[40]

* Ref. [41]; # Ref. [42]; % Ref. [43]; $ Ref. [28]; nd, not determined.

A tighter paracellular barrier was obtained in the hydrogel-based human corneal model in three weeks of culture, compared to in the cells grown conventionally in the inserts for four weeks (Table 2). In general, the cell layers grown in the inserts were more permeable (the range of P_{app} values was higher). Barrier characteristics are crucially important in in vitro models used for drug permeation studies. While establishing an in vitro model for assessing drug permeability, it is important to keep in mind the major layers responsible for limiting the penetration, both the corneal epithelium and stroma. The main barrier for the penetration of hydrophilic molecules is the corneal epithelium [1]. Thus, the human cornea is a naturally efficient barrier for different molecules due to its natural characteristics and cellular content.

The drug's ability to permeate through corneal barriers is linked to its molecular properties. Four properties strongly associated with the drug permeability: lipophilicity (logarithm of the octanol/water partition coefficient, LogP), number of hydrogen-bond donor groups, number of hydrogen-bond acceptor groups, polar surface area, and molecular weight. These are known as Lipiski's rule of five [44]. The same molecular properties have been shown to influence the in vitro P_{app} values across different cell models [45]. Sufficient lipophilicity is needed in order to be able to partition into the cell membrane. Lipophilicity also depends on the ionic attractive and repulsive interactions between the molecule and the partitioning phase (e.g., epithelial cell multilayer or collagen hydrogel); (lipophilicity = hydrophobicity − polarity + ionic interactions) [46].

Significant differences between the P_{app} values of the hydrogel-based human corneal mimetic and cells grown in inserts were observed (Table 3); FD4 and betaxolol were compounds that did not show statistically significant differences. Statistically significant differences can be explained by the fact that the corneal mimetic contains a stroma-like hydrophilic collagen hydrogel layer that is not present in a conventionally insert-grown corneal epithelial multilayer. The hydrophilic stroma layer creates a significant barrier for lipophilic molecules, such as dexamethasone, betaxolol, and rhodamine B (LogP 1.83, 2.81, and 2.3 (Table 2), respectively). Interestingly, the higher water content of the hydrogel compared to the human cornea (91.5% vs. 78%) did not decrease the P_{app} value of dexamethasone, betaxolol, and Rhodamine B, indicating that the higher water content does not limit the transport through the hydrogel-based human corneal mimetic.

Table 3. Statistical comparison of P_{app} values. Differences were considered to be statistically significant at $P < 0.05$. * $P < 0.05$; ** $P < 0.01$; *** $P < 0.001$; **** $P < 0.0001$; ns, not significant.

Test Molecule	Hydrogel-Based Human Corneal Model vs. Rabbit Corneal Permeability	Cells Grown in Inserts vs. Rabbit Corneal Permeability	Hydrogel-Based Human Corneal Model vs. Cells Grown in Inserts
FITC-dextran 70 kDa	0.0219 *	0.3789 ns	0.0077 **
FITC-dextran 4 kDa	0.0081 **	<0.0001 ****	0.0512 ns
Rhodamine 123	0.0044 **	<0.0001 ****	<0.0001 ****
6-carboxy-fluorescein	0.9956 ns	<0.0001 ****	<0.0001 ****
Brinzolamide	0.0650 ns	<0.0001 ****	<0.0001 ****
Dexamethasone	0.7991 ns	<0.0001 ****	<0.0001 ****
Chloramphenicol	0.0229 *	0.0002 ***	<0.0001 ****
Timolol maleate	0.0084 **	0.4509 ns	0.0488 *
Pilocarpine	0.8231 ns	<0.0001 ****	<0.0001 ****
Rhodamine B	0.0089 **	<0.0001 ****	<0.0001 ****
Betaxolol	0.2858 ns	0.0513 ns	0.1389 ns

In addition, there is a significant difference ($P < 0.0001$, Table 3) between the P_{app} value of pilocarpine in the hydrogel-based human corneal model ($16.86 \pm 0.58 \times 10^{-6}$ cm/s) and in the insert-grown corneal multilayer ($39.4 \pm 0.97 \times 10^{-6}$ cm/s). An unionized form of pilocarpine (approx. 50% at physiological pH [40]) has a P_{app} value across the cornea twice as high as that of the ionized form of pilocarpine [47]. Thus, a higher P_{app} value might be a result of more favorable partitioning of unionized pilocarpine in the insert-grown multilayer. On the contrary, the P_{app} value of timolol maleate is significantly higher ($P < 0.05$, Table 3) in the hydrogel-based human corneal model ($29.47 \pm 1.05 \times 10^{-6}$ cm/s) than in the insert-grown corneal multilayer ($20.62 \pm 4.27 \times 10^{-6}$ cm/s), resulting from the fact that only 1% of timolol maleate is unionized at physiological pH [40], and a significantly thicker epithelial multilayer in cells cultured on inserts forms a rate-limiting barrier.

Interestingly, the high-molecular-weight reference compound (FD70) exhibited a significantly higher P_{app} value ($P < 0.01$, Table 3) in the hydrogel-based corneal model than in the corneal cells grown in inserts. A much thicker multilayer of corneal cells grown in the inserts had an impact on the P_{app} value as the tight junctional proteins (ZO-1 and occludin) were shown to be expressed in the full thickness in both in vitro models (Figure 2). FD70 is a fully paracellularly transported molecule. Thus, the thicker multilayer with the expression of tight junctions in the full thickness decreased the P_{app} value efficiently.

Linear regression analysis showed an excellent relationship ($R^2 = 0.9297$) between permeability values across the in vitro corneal mimetic with hydrogel and rabbit cornea (Figure 3A) with a high Pearson's correlation coefficient ($r = 0.96$). This indicates that an in vitro corneal mimetic with a hydrogel layer correlates very well with P_{app} values obtained by measuring the rabbit corneal permeability ex vivo, and it can be used as a tool for drug permeability testing during drug development. However, the relationship between the permeability of the current in vitro standard (cells grown on cell culture inserts) and that of the rabbit cornea was found to be significantly lower ($R^2 = 0.7991$, $r = 0.89$) (Figure 3B).
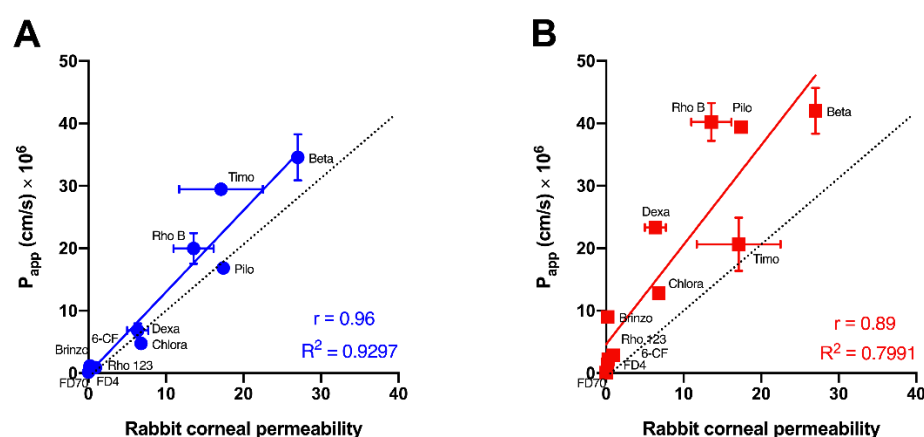
Figure 3. Linear regression between the apparent permeability coefficient, P_{app} (cm/s) $\times 10^6$, of ophthalmic drugs and reference molecules across in vitro hydrogel-based corneal mimetic (**A**), the human corneal cells grown conventionally in cell culture inserts (**B**), and rabbit corneal permeability values, respectively. The data refer to the mean $\pm$ SEM. Pearson's correlation coefficients (r) for the in vitro corneal mimetic with hydrogel and the cells grown in cell culture inserts were r = 0.96 and 0.89, respectively. The dotted lines in the figures represent a perfect positive correlation (r = 1). The goodness of the correlation fit (R^2 value) describes how well the corneal mimetic in vitro model agrees with the corresponding rabbit corneal permeability values.

This study further confirms that the human corneal in vitro mimetic requires a hydrophilic stroma-like structure in order to be able to reliably predict the permeability coefficients. Currently, there are available established corneal in vitro models having a hydrophilic stroma-like structure formed using rat tail collagen combined with keratocytes, stromal stem cells, and neuronal cells [8–10]. Together these studies verify the use of immortalized HCE-T cells suitable for permeability testing, although the HCE-T cells may not fully represent the in vivo cornea architecture or tight junctional localization (Figure 2), multidrug resistance-associated protein expressions [48], or cornea-specific differentiation markers [49].

Previously, human corneal cells have been grown on NHS/EDC crosslinked collagen hydrogels, and the diffusion permeability of high-molecular-weight (66 kDa) reference molecule was in the same range as in the present study [20]. In the same study, a reliable stability and integration of the hydrogel implant was demonstrated in rabbit and porcine corneas over the period of 6 months after the implantation [20]. However, no previous data on the permeability of different molecules across human corneal cells grown on collagen hydrogels crosslinked with NHS/EDC or DMTMM are available. Therefore, the present study provides the first systematic comparison of ophthalmic drug permeability between an in vitro hydrogel-based human corneal mimetic, human corneal epithelial cells grown conventionally in inserts, and the ex vivo gold standard, rabbit corneal permeability.

4. Conclusions

In this study, the successful development and testing of an efficient in vitro human corneal model, composed of two major layers of the cornea, containing both a stromal equivalent and epithelial cells, is described. The model is based on the human corneal epithelial cells multilayered on a type I collagen-based self-supporting hydrogel, which exhibits permeability that correlates very well to values obtained by measuring rabbit corneal permeability ex vivo. Therefore, we conclude that this in vitro human cornea mimetic can be used for drug permeability tests, whilst avoiding ethical issues and the higher expenses incurred.

References

1. Cholkar, K.; Patel, S.P.; Vadlapudi, A.D.; Mitra, A.K. Novel Strategies for Anterior Segment Ocular Drug Delivery. *J. Ocul. Pharmacol. Ther.* **2013**, *29*, 106–123. [CrossRef] [PubMed]
2. Mantelli, F.; Mauris, J.; Argüeso, P. The ocular surface epithelial barrier and other mechanisms of mucosal protection: From allergy to infectious diseases. *Curr. Opin. Allergy Clin. Immunol.* **2013**, *13*, 563–568. [CrossRef]
3. Directive of the European Parliament and of the Council on the Protection of Animals Used for Scientific Purposes. Directive 2010/63/EU. 2010. Available online: https://eur-lex.europa.eu/eli/dir/2010/63/oj (accessed on 10 January 2021).
4. Kouchak, M.; Bahmandar, R.; Bavarsad, N.; Farrahi, F. Ocular Dorzolamide Nanoliposomes for Prolonged IOP Reduction: In-vitro and in-vivo Evaluation in Rabbits. *Iran. J. Pharm. Res.* **2016**, *15*, 205–212. [PubMed]
5. Palma, S.D.; Tártara, L.I.; Quinteros, D.; Allemandi, D.A.; Longhi, M.R.; Granero, G.E. An efficient ternary complex of acetazolamide with HP-ß-CD and TEA for topical ocular administration. *J. Control. Release* **2009**, *138*, 24–31. [CrossRef] [PubMed]
6. Makhmalzadeh, B.S.; Salimi, A.; Niroomand, A. Loratadine-Loaded Thermoresponsive Hydrogel: Characterization and Ex-vivo Rabbit Cornea Permeability Studies. *Iran. J. Pharm. Res.* **2018**, *17*, 460–469.
7. Kaluzhny, Y.; Kinuthia, M.W.; Truong, T.; Lapointe, A.M.; Hayden, P.; Klausner, M. New Human Organotypic Corneal Tissue Model for Ophthalmic Drug Delivery Studies. *Investig. Opthalmol. Vis. Sci.* **2018**, *59*, 2880–2898. [CrossRef]
8. Wang, S.; Ghezzi, C.E.; Gomes, R.; Pollard, R.E.; Funderburgh, J.L.; Kaplan, D.L. In vitro 3D corneal tissue model with epithelium, stroma, and innervation. *Biomaterials* **2017**, *112*, 1–9. [CrossRef]
9. Hahne, M.; Zorn-Kruppa, M.; Guzman, G.; Brandner, J.M.; Haltner-Ukomado, E.; Wätzig, H.; Reichl, S. Prevalidation of a Human Cornea Construct as an Alternative to Animal Corneas for In Vitro Drug Absorption Studies. *J. Pharm. Sci.* **2012**, *101*, 2976–2988. [CrossRef]
10. Hahne, M.; Reichl, S. Development of a serum-free human cornea construct for in vitro drug absorption studies: The influence of varying cultivation parameters on barrier characteristics. *Int. J. Pharm.* **2011**, *416*, 268–279. [CrossRef]
11. Yamaguchi, H.; Takezawa, T. Fabrication of a Corneal Model Composed of Corneal Epithelial and Endothelial Cells via a Collagen Vitrigel Membrane Functioned as an Acellular Stroma and Its Application to the Corneal Permeability Test of Chemicals. *Drug Metab. Dispos.* **2018**, *46*, 1684–1691. [CrossRef]
12. Chang, J.-E.; Basu, S.K.; Lee, V.H.L. Air-interface condition promotes the formation of tight corneal epithelial cell layers for drug transport studies. *Pharm. Res.* **2000**, *17*, 670–676. [CrossRef]
13. Scholz, M.; Lin, J.-E.C.; Lee, V.H.L.; Keipert, S. Pilocarpine Permeability across Ocular Tissues and Cell Cultures: Influence of Formulation Parameters. *J. Ocul. Pharmacol. Ther.* **2002**, *18*, 455–468. [CrossRef]
14. Reichl, S.; Kölln, C.; Hahne, M.; Verstraelen, J. In vitro cell culture models to study the corneal drug absorption. *Expert Opin. Drug Metab. Toxicol.* **2011**, *7*, 559–578. [CrossRef]
15. Almubrad, T.; Akhtar, S. Structure of corneal layers, collagen fibrils, and proteoglycans of tree shrew cornea. *Mol. Vis.* **2011**, *17*, 2283–2291.
16. Ihanamäki, T.; Pelliniemi, L.J.; Vuorio, E. Collagens and collagen-related matrix components in the human and mouse eye. *Prog. Retin. Eye Res.* **2004**, *23*, 403–434. [CrossRef] [PubMed]
17. Korjamo, T.; Heikkinen, A.; Waltari, P.; Mönkkönen, J. The Asymmetry of the Unstirred Water Layer in Permeability Experiments. *Pharm. Res.* **2008**, *25*, 1714–1722. [CrossRef] [PubMed]

18. Jansen, K.A.; Donato, D.M.; Balcioglu, H.E.; Schmidt, T.; Danen, E.H.; Koenderink, G.H. A guide to mechanobiology: Where biology and physics meet. *Biochim. Biophys. Acta (BBA) Bioenerg.* **2015**, *1853*, 3043–3052. [CrossRef] [PubMed]

19. Fagerholm, P.; Lagali, N.S.; Ong, J.A.; Merrett, K.; Jackson, W.B.; Polarek, J.W.; Suuronen, E.J.; Liu, Y.; Brunette, I.; Griffith, M. Stable corneal regeneration four years after implantation of a cell-free recombinant human collagen scaffold. *Biomaterials* **2014**, *35*, 2420–2427. [CrossRef] [PubMed]

20. Liu, Y.; Gan, L.; Carlsson, D.J.; Fagerholm, P.; Lagali, N.; Watsky, M.A.; Munger, R.; Hodge, W.G.; Priest, D.; Griffith, M. A Simple, Cross-linked Collagen Tissue Substitute for Corneal Implantation. *Investig. Opthalmol. Vis. Sci.* **2006**, *47*, 1869–1875. [CrossRef]

21. Liu, W.; Deng, C.; McLaughlin, C.R.; Fagerholm, P.; Lagali, N.; Heyne, B.; Scaiano, J.; Watsky, M.A.; Kato, Y.; Munger, R.; et al. Collagen–phosphorylcholine interpenetrating network hydrogels as corneal substitutes. *Biomaterials* **2009**, *30*, 1551–1559. [CrossRef] [PubMed]

22. Haagdorens, M.; Cėpla, V.; Melsbach, E.; Koivusalo, L.; Skottman, H.; Griffith, M.; Valiokas, R.; Zakaria, N.; Pintelon, I.; Tassignon, M.-J. In Vitro Cultivation of Limbal Epithelial Stem Cells on Surface-Modified Crosslinked Collagen Scaffolds. *Stem Cells Int.* **2019**, *2019*, 7867613. [CrossRef] [PubMed]

23. Domke, J.; Radmacher, M. Measuring the Elastic Properties of Thin Polymer Films with the Atomic Force Microscope. *Langmuir* **1998**, *14*, 3320–3325. [CrossRef]

24. Sokolov, I.; Dokukin, M.E.; Guz, N.V. Method for quantitative measurements of the elastic modulus of biological cells in AFM indentation experiments. *Methods* **2013**, *60*, 202–213. [CrossRef]

25. Hutter, J.L.; Bechhoefer, J. Calibration of atomic-force microscope tips. *Rev. Sci. Instrum.* **1993**, *64*, 1868–1873. [CrossRef]

26. Araki-Sasaki, K.; Ohashi, Y.; Sasabe, T.; Hayashi, K.; Watanabe, H.; Tano, Y.; Handa, H. An SV40-immortalized human corneal epithelial cell line and its characterization. *Investig. Ophthalmol. Vis. Sci.* **1995**, *36*, 614–621.

27. Hakkarainen, J.J.; Reinisalo, M.; Ragauskas, S.; Seppänen, A.; Kaja, S.; Kalesnykas, G. Acute cytotoxic effects of marketed ophthalmic formulations on human corneal epithelial cells. *Int. J. Pharm.* **2016**, *511*, 73–78. [CrossRef]

28. Toropainen, E.; Ranta, V.P.; Talvitie, A.; Suhonen, P.; Urtti, A. Culture model of human corneal epithelium for prediction of ocular drug absorption. *Investig. Ophthalmol. Vis. Sci.* **2001**, *42*, 2942–2948.

29. D'Este, M.; Eglin, D.; Alini, M. A systematic analysis of DMTMM vs EDC/NHS for ligation of amines to Hyaluronan in water. *Carbohydr. Polym.* **2014**, *108*, 239–246. [CrossRef]

30. Balion, Z.; Cėpla, V.; Svirskiene, N.; Svirskis, G.; Druceikaitė, K.; Inokaitis, H.; Rusteikaitė, J.; Masilionis, I.; Stankevičienė, G.; Jelinskas, T.; et al. Cerebellar Cells Self-Assemble into Functional Organoids on Synthetic, Chemically Crosslinked ECM-Mimicking Peptide Hydrogels. *Biomolecules* **2020**, *10*, 754. [CrossRef]

31. Taylor, Z.D.; Garritano, J.; Sung, S.; Bajwa, N.; Bennett, D.B.; Nowroozi, B.; Tewari, P.; Sayre, J.W.; Hubschman, J.-P.; Deng, S.X.; et al. THz and mm-Wave Sensing of Corneal Tissue Water Content: In Vivo Sensing and Imaging Results. *IEEE Trans. Terahertz Sci. Technol.* **2015**, *5*, 184–196. [CrossRef] [PubMed]

32. Qin, X.; Tian, L.; Zhang, H.; Chen, X.; Li, L. Evaluation of corneal elastic modulus based on Corneal Visualization Scheimpflug Technology. *Biomed. Eng. Online* **2019**, *18*, 42. [CrossRef] [PubMed]

33. Welsh, C.; Gay, S.; Rhodes, R.; Pfister, R.; Miller, E.J. Collagen heterogeneity in normal rabbit cornea. I. Isolation and biochemical characterization of the genetically-distinct collagens. *Biochim. Biophys. Acta (BBA) Protein Struct.* **1980**, *625*, 78–88. [CrossRef]

34. Kimura, K.; Mori, T.; Hadachi, H.; Saito, T.; Nishida, T.; Kawano, S.; Inoue, J. Quantitative Analysis of the Effects of Extracellular Matrix Proteins on Membrane Dynamics Associated with Corneal Epithelial Cell Motility. *Investig. Opthalmol. Vis. Sci.* **2010**, *51*, 4492–4499. [CrossRef] [PubMed]

35. Wu, P.; Gong, H.; Richman, R.; Freddo, T.F. Localization of occludin, ZO-1, and pan-cadherin in rabbit ciliary epithelium and iris vascular endothelium. *Histochem. Cell Biol.* **2000**, *114*, 303–310. [CrossRef]

36. Huang, A.J.; Tseng, S.C.; Kenyon, K.R. Paracellular permeability of corneal and conjunctival epithelia. *Investig. Ophthalmol. Vis. Sci.* **1989**, *30*, 684–689.

37. Sasaki, H.; Yamamura, K.; Tei, C.; Nishida, K.; Nakamura, J. Ocular Permeability of FITC-Dextran with Absorption Promoter for Ocular Delivery of Peptide Drug. *J. Drug Target.* **1995**, *3*, 129–135. [CrossRef]

38. Becker, U.; Ehrhardt, C.; Daum, N.; Baldes, C.; Schaefer, U.F.; Ruprecht, K.W.; Kim, K.-J.; Lehr, C.-M. Expression of ABC-Transporters in Human Corneal Tissue and the Transformed Cell Line, HCE-T. *J. Ocul. Pharmacol. Ther.* **2007**, *23*, 172–181. [CrossRef]

39. Schoenwald, R.D. Ocular Drug Delivery. *Clin. Pharmacokinet.* **1990**, *18*, 255–269. [CrossRef]

40. Prausnitz, M.R.; Noonan, J.S. Permeability of cornea, sclera, and conjunctiva: A literature analysis for drug delivery to the eye. *J. Pharm. Sci.* **1998**, *87*, 1479–1488. [CrossRef]

41. National Center for Biotechnology Information. PubChem Compound Summary. 2021. Available online: https://pubchem.ncbi.nlm.nih.gov/ (accessed on 13 February 2021).

42. Tomita, M.; Menconi, M.J.; Delude, R.L.; Fink, M.P. Polarized transport of hydrophilic compounds across rat colonic mucosa from serosa to mucosa is temperature dependent. *Gastroenterology* **2000**, *118*, 535–543. [CrossRef]

43. Duvvuri, M.; Gong, Y.; Chatterji, D.; Krise, J.P. Weak Base Permeability Characteristics Influence the Intracellular Sequestration Site in the Multidrug-resistant Human Leukemic Cell Line HL-60. *J. Biol. Chem.* **2004**, *279*, 32367–32372. [CrossRef]

44. Lipinski, C.A.; Lombardo, F.; Dominy, B.W.; Feeney, P.J. Experimental and computational approaches to estimate solubility and permeability in drug discovery and development settings. *Adv. Drug Deliv. Rev.* **2001**, *46*, 3–26. [CrossRef]

45. Hakkarainen, J.J.; Pajander, J.; Laitinen, R.; Suhonen, M.; Forsberg, M. Similar molecular descriptors determine the in vitro drug permeability in endothelial and epithelial cells. *Int. J. Pharm.* **2012**, *436*, 426–443. [CrossRef]

46. Liu, X.; Testa, B.; Fahr, A. Lipophilicity and Its Relationship with Passive Drug Permeation. *Pharm. Res.* **2010**, *28*, 962–977. [CrossRef]

47. Mitra, A.K.; Mikkelson, T.J. Mechanism of Transcorneal Permeation of Pilocarpine. *J. Pharm. Sci.* **1988**, *77*, 771–775. [CrossRef]

48. Verstraelen, J.; Reichl, S. Multidrug Resistance-Associated Protein (MRP1, 2, 4 and 5) Expression in Human Corneal Cell Culture Models and Animal Corneal Tissue. *Mol. Pharm.* **2014**, *11*, 2160–2171. [CrossRef]

49. Rubelowski, A.-K.; Latta, L.; Katiyar, P.; Stachon, T.; Käsmann-Kellner, B.; Seitz, B.; Szentmáry, N. HCE-T cell line lacks cornea-specific differentiation markers compared to primary limbal epithelial cells and differentiated corneal epithelium. *Graefe's Arch. Clin. Exp. Ophthalmol.* **2020**, *258*, 565–575. [CrossRef]